TELKOMNIKA Telecommunication, Computing, Electronics and Control
Vol. 19, No. 1, February 2021, pp. 19~26
ISSN: 1693-6930, accredited First Grade by Kemenristekdikti, Decree No: 21/E/KPT/2018
DOI: 10.12928/TELKOMNIKA.v19i1.15861

Performance of downlink NOMA with multiple antenna base station, full-duplex and D2D transmission

Minh-Sang Van Nguyen[1], Dinh-Thuan Do[2]
[1]Industrial University of Ho Chi Minh City (IUH), Ho Chi Minh City, Vietnam
[2]Wireless Communications Research Group, Faculty of Electrical & Electronics Engineering,
Ton Duc Thang University, Ho Chi Minh City, Vietnam

Article Info

Article history:

Received Feb 17, 2020
Revised May 5, 2020
Accepted May 14, 2020

Keywords:

Full-duplex
Non-orthogonal multiple access
Transmit antenna selection

ABSTRACT

The implementation of non-orthogonal multiple access (NOMA) and transmit antenna selection (TAS) technique has considered in this paper since TAS-aware base station (BS) provides the low cost, low complexity, and high diversity gains. In this paper, we investigate performance of two users by deriving outage probability. The system performance benefits from design of TAS and full-duplex (FD) scheme applied at NOMA users, and bandwidth efficiency will be enhanced although self-interference exists due to FD. The main contribution lies in the exact expressions of outage probability which are derived to exhibit system performance. Different from the simulated parameters, the analytical results show that increasing number of transmit antennas at the BS is way to improve system performance.

Corresponding Author:

Dinh-Thuan Do
Wireless Communications Research Group
Faculty of Electrical & Electronics Engineering
Ton Duc Thang University
Ho Chi Minh City, Vietnam
Email: dodinhthuan@tdtu.edu.vn

1. INTRODUCTION

Non-orthogonal multiple access (NOMA) is known as a promising candidate providing ability of multiple access to massive users in next generation communications [1-4]. The higher the spectral efficiency and user fairness are beneficial from employing NOMA in emerging wireless communication networks. NOMA technique has been indicated that it is capable of combining with many wireless communication techniques due to its superior spectral efficiency, and enhancing the system performance. For example, the technique of cooperative transmission applied together with NOMA is suitable with a multi-user environment [5-10]. Therefore, the cooperative transmission for NOMA can improve the communication reliability for the users who are in poor channels [11-17].

Besides NOMA, multiple-input multiple-output (MIMO) technology benefits network reliability and capacity [18, 19]. However, the computational complexity and power consumption are disadvantage of such MIMO NOMA scheme since multiple antennas result in the increased cost [20]. The transmit antenna selection (TAS) has been applied as a practical solution to avoid the undesirable effects the simultaneous use of multiple antennas [21]. The authors in [22] indicated that TAS techniques possessing full diversity gain. TAS and NOMA are introduced in recent papers [23-25]. For example, NOMA was studied in [23] by employing transmit antenna selection (TAS) at the base Station to show the outage performance for downlink.

Notation:
The cumulative distribution function of a real-valued random variable X is denoted by $F_X(.)$ and $f_X(.)$ stands for probability density functions. $Pr(.)$ is probability function.

2. SYSTEM MODE

Consider a downlink of network as shown in Figure 1. The base station (BS) equipped many antennas to improve performance of far users, i.e. two NOMA users. In this case, main object of this paper is full-duplex (FD) mode is enabled at two NOMA users ($D_i, i = \{1,2\}$) which operate in device-to-device (D2D), two NOMA users can communicate directly without helping of the BS which has K antennas. The complex channel coefficients for the links $BS \to D_1$, $BS \to D_2$, $D_1 \to D_1$, $D_2 \to D_2$, $D_2 \to D_1$,$D_1 \to D_2$ are represented by $|h_{k,1}|^2 \sim CN(0, \lambda_1)$, $|h_{k,2}|^2 \sim CN(0, \lambda_2)$, $|l_1|^2 \sim CN(0, \lambda_3)$, $|l_2|^2 \sim CN(0, \lambda_4)$, $|g_1|^2 \sim CN(0, \lambda_5)$, $|g_2|^2 \sim CN(0, \lambda_6)$, respectively. Further, in this scenario NOMA users are double-antenna devices and operate in a FD mode, except for the BS equipped multiple antenna. The direct links between the source node and the users are assumed available which is common in the scenarios where two NOMA users acquire device to device transmission. We assume that all users are clustered very close such that a homogeneous network topology is considered in our paper. The channels associated with each link exhibit Rayleigh fading and additive white Gaussian noise (AWGN).

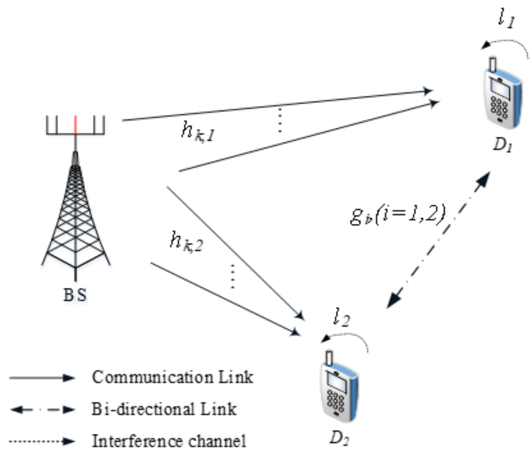

Figure 1. System model of NOMA downlink

In first phase, the BS communicates with two users with signal $x_i = \sqrt{a_1 P_S} x_1 + \sqrt{a_2 P_S} x_2$ to D_1 and D_2 according to direct transmissions. Where P_S is the transmitted power of the BS, x_i is the signal of D_i, and a_1, a_2 is the power allocation coefficient with $a_1 + a_2 = 1$, $a_1 > a_2$. In FD mode, user D_i receives the superposed signal and loop interference signal simultaneously, the received signal at D_i is

$$y_{Di} = h_{k,i} x_i + l_i \sqrt{\varpi P_{Di}} x_I + w_i; i \in (1,2) \quad (1)$$

where ϖ denotes user 1 working in FD. w_i is the additive white Gaussian noise with zero mean and variance N_0. The LI is modeled as a Rayleigh fading channel with coefficient l_i. We call x_I as signal related to self-interference at D_i. P_{Di} are the normalized transmission powers at D_i.

Then, the received signal-to-interference-plus-noise ratio (SINR) at user 1 become

$$\gamma_{SD1,k} = \frac{a_1 \rho |h_{k,1}|^2}{a_2 \rho |h_{k,1}|^2 + \varpi \rho |l_1|^2 + 1} \quad (2)$$

where $\rho = P_S / N_0$ is the transmit signal-to-noise ratio (SNR) which was measured at the BS. In this scenario, D_2 is so-called as the successive interference cancellation (SIC) user, i.e. SIC is required to eliminate interference from signal of D_1. Firtly, the received SINR at user 2 to detect user1's message x_1 is given by

$$\gamma_{SD1\leftarrow 2,k} = \frac{a_1\rho|h_{k,2}|^2}{a_2\rho|h_{k,2}|^2+\varpi\rho|l_2|^2+1} \tag{3}$$

Then SIC activated to eliminate interference from D_1, the received SINRs at the D_2 is calculated to decode its own signal as

$$\gamma_{SD2,k} = \frac{a_2\rho|h_{k,2}|^2}{\varpi\rho|l_2|^2+1} \tag{4}$$

In this phase, the cooperation signal is transmitted from the user with a stronger channel gain to the user with a weaker gain. The cooperation signal can help D_1 to decode its data, or D_2 to perform SIC better. The cooperation siganl received by D_1 is given by

$$f_{Di} = g_i\sqrt{P_S}s + l_i\sqrt{\varpi P_{Di}}x_I + w_i \tag{5}$$

Generally, the received SINR at user i is given by

$$\gamma_{Di} = \frac{\rho|g_i|^2}{\varpi\rho|l_i|^2+1} \tag{6}$$

The antenna index can be selected to strengthen the BS to serve user i link as follows

$$k *= arg \underbrace{max}_{k=1,\dots,K}\left(|h_{k,i}|^2\right) \tag{7}$$

In this case, CDF and PDF related selected channel are given by [26, 27]

$$\begin{aligned} F_{|h_{k*,i}|^2}(x) &= \left(1-\exp\left(-\frac{x}{\lambda_{hki}}\right)\right)^K \\ &= 1-\sum_{k=1}^{K}\binom{K}{k}(-1)^{k-1}\exp\left(-\frac{kx}{\lambda_{hki}}\right) \end{aligned} \tag{8}$$

and

$$\begin{aligned} f_{|h_{k*,i}|^2}(x) &= K\left[F_{|h_{1,i}|^2}(x)\right]^{K-1} f_{|h_{1,i}|^2}(x) \\ &= \sum_{k=1}^{K}\binom{K}{k}(-1)^{k-1}\frac{k}{\lambda_{hki}}\exp\left(-\frac{kx}{\lambda_{hki}}\right) \end{aligned} \tag{9}$$

3. OUTAGE PROBABILITY

When the targeted data rates, R_1 and R_2, are determined by the users' QoS requirements for user i. In fact, the outage probability is an important performance criterion which need be investigated. If the outage event occurs at the non-SIC user, the SIC user does not use the cooperation signal, and the outage of the SIC user does not allow the cooperation from the SIC user to the non-SIC user.

3.1. Outage probability of user

Outage Probability of D_1: According to NOMA protocol, the complementary events of outage at D_1 can be explained as: D_1 can detect x_2 as well as its own message x_1. From the above description, the outage probability of D_1 is expressed as

$$\begin{aligned} OP_{D1} &= \Pr\left(\max\left(\gamma_{SD1,k^*},\gamma_{D1}\right)<\gamma_1\right) \\ &= \Pr\left(\gamma_{SD1,k^*}<\gamma_1,\gamma_{D1}<\gamma_1\right) \\ &= \underbrace{\Pr\left(\gamma_{SD1,k^*}<\gamma_1\right)}_{\Omega_1}\times\underbrace{\Pr\left(\gamma_{D1}<\gamma_1\right)}_{\Omega_2}, \end{aligned} \tag{10}$$

where $\gamma_i = 2^{R_i} - 1, (i = 1,2)$, R_i is target rate for signal x_i, with the help of (2) and (3), then it can be calculated the terms Ω_1 and Ω_2 as

$$\begin{aligned} \Omega_1 &= 1-\Pr\left(\gamma_{SD1,k^*}\ge\gamma_1\right) \\ &= 1-\Pr\left(\left|h_{k^*,1}\right|^2\ge\frac{\gamma_1\left(\varpi\rho\left|l_1\right|^2+1\right)}{\rho\left(a_1-\gamma_1 a_2\right)}\right) \\ &= 1-\int_0^\infty\left(1-F_{\left|h_{k^*,1}\right|^2}\left(\frac{\gamma_1\left(\varpi\rho x+1\right)}{\rho\left(a_1-\gamma_1 a_2\right)}\right)\right)f_{\left|l_1\right|^2}\left(x\right)dx. \end{aligned} \tag{11}$$

From (8) and (9), it can be computed Ω_2 as

$$\begin{aligned} \Omega_2 &= 1-\int_0^\infty\exp\left(-\frac{\gamma_1\left(\varpi\rho x+1\right)}{\rho\lambda_5}\right)\frac{1}{\lambda_3}\exp\left(-\frac{x}{\lambda_3}\right)dx \\ &= 1-\frac{1}{\lambda_3}\exp\left(-\frac{\gamma_1}{\rho\lambda_5}\right)\int_0^\infty\exp\left(-\left(\frac{\gamma_1\varpi}{\lambda_5}+\frac{1}{\lambda_3}\right)x\right)dx \\ &= 1-\frac{\lambda_5}{\gamma_1\varpi\lambda_3+\lambda_5}\exp\left(-\frac{\gamma_1}{\rho\lambda_5}\right). \end{aligned} \tag{12}$$

Plugging (11), (13), into (10), the final result can be obtained as

$$\begin{aligned} OP_{D1} &= \left(1-\sum_{k=1}^{K}\binom{K}{k}\left(-1\right)^{k-1}\frac{\left(a_1-\gamma_1 a_2\right)\lambda_1}{k\gamma_1\varpi\lambda_3+\left(a_1-\gamma_1 a_2\right)\lambda_1}\exp\left(-\frac{k\gamma_1}{\left(a_1-\gamma_1 a_2\right)\rho\lambda_1}\right)\right) \\ &\quad\times\left(1-\frac{\rho\lambda_5}{\gamma_1\varpi\rho\lambda_3+\rho\lambda_5}\exp\left(-\frac{\gamma_1}{\rho\lambda_5}\right)\right). \end{aligned} \tag{13}$$

3.2. Outage probability of user 2

The outage events of D_2 can be explained as below. The first is that D_1 cannot detect x_2. The second is that D_2 cannot detect its own message x_2 on the conditions that D_1 can detect x_2 successfully. Based on these, the outage probability of D_2 is expressed as

$$\begin{aligned} OP_{D2} &= \Pr\left(\max\left(\min\left(\gamma_{SD1\leftarrow 2,k^*},\gamma_{SD2,k^*}\right),\gamma_{D2}\right)<\gamma_2\right) \\ &= \Pr\left(\min\left(\gamma_{SD1\leftarrow 2,k^*},\gamma_{SD2,k^*}\right)<\gamma_2,\gamma_{D2}<\gamma_2\right) \\ &= \underbrace{\Pr\left(\min\left(\gamma_{SD1\leftarrow 2,k^*},\gamma_{SD2,k^*}\right)<\gamma_2\right)}_{\Gamma_1}\times\underbrace{\Pr\left(\gamma_{D2}<\gamma_2\right)}_{\Gamma_2}. \end{aligned} \tag{14}$$

From (14), Γ_1 is given by

$$\begin{aligned}\Gamma_1 &= 1-\Pr\left(\left|h_{k^*,2}\right|^2 \geq \theta\left(\varpi\rho\left|l_2\right|^2+1\right)\right) \\ &= 1-\int_0^\infty \left(1-F_{\left|h_{k^*,2}\right|^2}\left(\theta\left(\varpi\rho x+1\right)\right)\right) f_{\left|l_2\right|^2}\left(x\right)dx,\end{aligned} \tag{15}$$

where $\theta = max\left(\frac{\gamma_2}{(a_1-\gamma_{th2}a_2)\rho}, \frac{\gamma_2}{a_2\rho}\right)$. From (8), Γ_1 can be expressed

$$\begin{aligned}\Gamma_1 &= 1-\sum_{k=1}^{K}\binom{K}{k}(-1)^{k-1}\frac{1}{\lambda_4}\exp\left(-\frac{k\theta}{\lambda_2}\right)\int_0^\infty \exp\left(-\left(\frac{k\theta\varpi\rho}{\lambda_2}+\frac{1}{\lambda_4}\right)x\right)dx \\ &= 1-\sum_{k=1}^{K}\binom{K}{k}(-1)^{k-1}\frac{\lambda_2}{k\theta\varpi\rho\lambda_4+\lambda_2}\exp\left(-\frac{k\theta}{\lambda_2}\right).\end{aligned} \tag{16}$$

From (14), Γ_2 is given by

$$\begin{aligned}\Gamma_2 &= 1-\Pr\left(\left|g_2\right|^2 \geq \frac{\gamma_2\left(\varpi\rho\left|l_2\right|^2+1\right)}{\rho}\right) \\ &= 1-\int_0^\infty \left(1-F_{\left|g_2\right|^2}\left(\frac{\gamma_2\left(\varpi\rho x+1\right)}{\rho}\right)\right) f_{\left|l_2\right|^2}\left(x\right)dx \\ &= 1-\frac{1}{\lambda_4}\exp\left(-\frac{\gamma_2}{\rho\lambda_6}\right)\int_0^\infty \exp\left(-\left(\frac{\gamma_2\varpi}{\lambda_6}+\frac{1}{\lambda_4}\right)x\right)dx \\ &= 1-\frac{\lambda_6}{\gamma_2\varpi\lambda_4+\lambda_6}\exp\left(-\frac{\gamma_2}{\rho\lambda_6}\right).\end{aligned} \tag{17}$$

Plugging (16), (17), into (14), the final result can be obtained as

$$\begin{aligned}OP_{D2} &= \left(1-\sum_{k=1}^{K}\binom{K}{k}(-1)^{k-1}\frac{\lambda_2}{k\theta\varpi\rho\lambda_4+\lambda_2}\exp\left(-\frac{k\theta}{\lambda_2}\right)\right) \\ &\times\left(1-\frac{\lambda_6}{\gamma_2\varpi\lambda_4+\lambda_6}\exp\left(-\frac{\gamma_2}{\rho\lambda_6}\right)\right).\end{aligned} \tag{18}$$

4. THE IMPERFECT SIC AT USER 2

Conversely, by considering imperfect SIC, the received SINRs at both D_2 become:

$$\gamma_{SD2,k}^{ip} = \frac{a_2\rho\left|h_{k,2}\right|^2}{a_1\rho\left|\tilde{h}_{k,1}\right|^2+\varpi\rho|l_2|^2+1} \tag{19}$$

where $\tilde{h}_{k,1} \sim CN(0, \vartheta\lambda_7)$, and the parameter $\vartheta(0 \leq \vartheta \leq 1)$ denotes the level of residual interference because of SIC imperfection at user 2. As a particular case, $\vartheta = 0$ and $\vartheta = 1$ represent perfect SIC and without SIC, respectively. The outage probability the user 2 is given by

$$\begin{aligned}OP_{D2}^{ip} &= \Pr\left(\max\left(\gamma_{SD2,k^*}^{ip}, \gamma_{Di}\right) < \gamma_2\right) \\ &= \Pr\left(\gamma_{SD2,k^*}^{ip} < \gamma_2, \gamma_{Di} < \gamma_2\right) \\ &= \underbrace{\Pr\left(\gamma_{SD2,k^*}^{ip} < \gamma_2\right)}_{\Phi_1}\times\underbrace{\Pr\left(\gamma_{Di} < \gamma_2\right)}_{\Phi_2}.\end{aligned} \tag{20}$$

From (22), Φ_1 is given by

$$\begin{aligned}\Phi_1 &= 1-\Pr\left(\left|h_{k^*,2}\right|^2 \geq \frac{\gamma_2\left(a_1\rho\left|h_{k^*,1}\right|^2+\varpi\rho\left|l_2\right|^2+1\right)}{a_2\rho}\right) \\ &= 1-\int_0^\infty\int_0^\infty\left(1-F_{\left|h_{k^*,2}\right|^2}\left(\frac{\gamma_2\left(a_1\rho x+\varpi\rho y+1\right)}{a_2\rho}\right)\right)f_{\left|h_{k^*,1}\right|^2}(x)\,dx f_{\left|l_2\right|^2}(y)\,dy.\end{aligned} \tag{21}$$

From (8), Φ_1 can be expressed

$$\begin{aligned}\Phi_1 &= 1-\sum_{k=1}^{K}\sum_{n=1}^{K}\binom{K}{k}\binom{K}{n}(-1)^{k+n-2}\frac{n}{\lambda_7}\frac{1}{\lambda_4}\exp\left(-\frac{k\gamma_2}{a_2\rho\lambda_2}\right) \\ &\times\int_0^\infty\int_0^\infty\exp\left(-\frac{k\gamma_2\left(a_1x+\varpi y\right)}{a_2\lambda_2}\right)\exp\left(-\frac{nx}{\lambda_7}\right)dx\exp\left(-\frac{y}{\lambda_4}\right)dy \\ &= 1-\sum_{k=1}^{K}\sum_{n=1}^{K}\binom{K}{k}\binom{K}{n}(-1)^{k+n-2}\frac{n}{\lambda_7}\frac{1}{\lambda_4}\exp\left(-\frac{k\gamma_2}{a_2\rho\lambda_2}\right) \\ &\times\int_0^\infty\exp\left(-\left(\frac{k\gamma_2a_1}{a_2\lambda_2}+\frac{n}{\lambda_7}\right)x\right)dx\int_0^\infty\exp\left(-\left(\frac{k\gamma_2\varpi}{a_2\lambda_2}+\frac{1}{\lambda_4}\right)y\right)dy \\ &= 1-\sum_{k=1}^{K}\sum_{n=1}^{K}\binom{K}{k}\binom{K}{n}(-1)^{k+n-2}\frac{na_2\lambda_2}{k\gamma_2a_1\lambda_7+a_2\lambda_2}\frac{a_2\lambda_2}{k\gamma_2\varpi\lambda_4+a_2\lambda_2}\exp\left(-\frac{k\gamma_2}{a_2\rho\lambda_2}\right).\end{aligned} \tag{22}$$

Φ_2 is calculated as Γ_2. From (17) and (22), OP_{D2}^{ip} is given by

$$\begin{aligned}OP_{D2}^{ip} &= \left(1-\sum_{k=1}^{K}\sum_{n=1}^{K}\binom{K}{k}\binom{K}{n}(-1)^{k+n-2}\frac{na_2\lambda_2}{k\gamma_2a_1\lambda_7+a_2\lambda_2}\frac{a_2\lambda_2}{k\gamma_2\varpi\lambda_4+a_2\lambda_2}\exp\left(-\frac{k\gamma_2}{a_2\rho\lambda_2}\right)\right) \\ &\times\left(1-\frac{\lambda_6}{\gamma_2\varpi\lambda_4+\lambda_6}\exp\left(-\frac{\gamma_2}{\rho\lambda_6}\right)\right).\end{aligned} \tag{23}$$

5. NUMERICAL RESULTS

In this section, numerical examples are performed to verify the outage performance of the downlink multiple-input-single-output (MISO) NOMA network under Rayleigh fading channels with FD scheme. Moreover, Monte-Carlo simulation is run in 106 times to compare with analytical results as proved formula presented in previous section. In Table 1 as shown in simulation parameters. In Figure 2, the outage probability versus transmit SNR at the BS ρ is presented in different power allocation parameters. We distance between BS and $D_i, (i = 1,2)$ is d_i , channel gain $\lambda_i = d_i^{-\alpha}$, $R_1 = 0.5, R_2 = 2$, the number of antenna at BS is $K = 2$. As clear observation, the exact analytical results and simulation results are in excellent agreement, and such outage probability will be constant at high-SNR regimes. Moreover, as the transmit SNR increases, the outage probability decreases Another important observation is that the outage probability for D_2 outperforms User 1. Figure 3 shows outage performance for user 1. The parameters for this case $a_1 = 0.7$,$R_2 = 2$, $K = 2$. It can be seen that lower target rate R_1 results in better outage performance.

In Figure 4, the outage probabilities are shown as a function of the transmit SNR. Reported from the impact of target rate R_2, there is a decrease in outage probability for such user as change to lower level of R_2This Figure requires several parameters as $a_1 = 0.7$,$R_1 = 0.5$, $K = 2$. Figure 5 plots the outage probability versus SNR with the different number of transmit antenna at the BS (other parameters as declarations in Figure 5 as $a_1 = 0.7$, $R_1 = 0.5$, $R_2 = 2$. More antenna at the BS indicates better outage probability in such NOMA. $K = 5$ case is best performance as important observation in this study

Table 1. Simulation parameters [28]

Parameter	Value
Node distances d_1, d_2, respectively	0.4, 0.2
Path loss exponent α	2
Power allocation factors a_1	0.6, 0.7, 0.8
$\lambda_3 = \lambda_4 = \lambda_7, \lambda_5 = \lambda_6$	0.01, 1
Outage threshold R_1; R_2	(0.2, 0.5); (1, 2)
Number of antenna K	2, 5
Transmit SNR ρ	0 to 40 dB

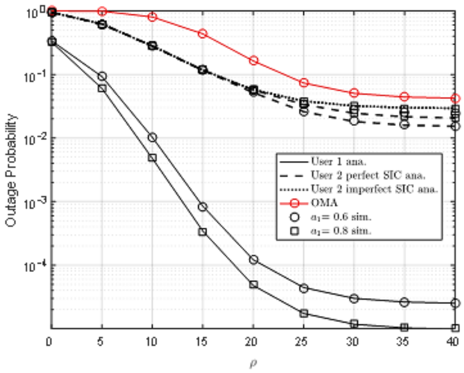

Figure 2. Outage performance of D_i, $(i = 1,2)$ and OMA versus ρ as varying a_1.

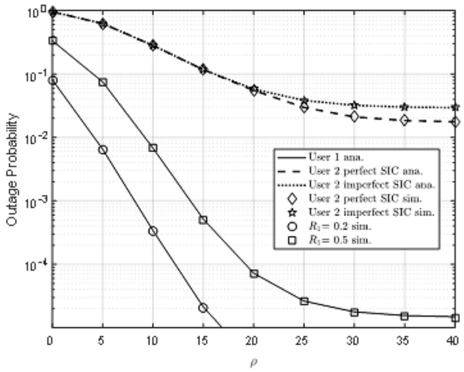

Figure 3. Outage performance of D_1 as varying R_1.

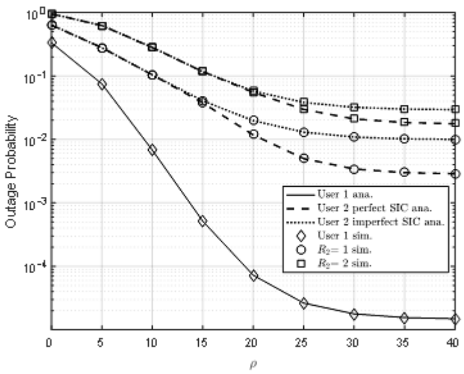

Figure 4. Outage performance of D_2 versus ρ as varying R_2.

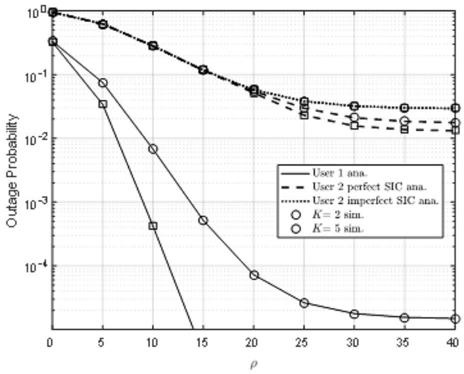

Figure 5. Outage performance of D_1 and D_2 as varying K.

6. CONCLUSION

This paper investigated analytically the impact of residual interference due to full-duplex scheme on users in downlink of NOMA. Closed-form analytical expressions for the outage probability were obtained. Our theoretical analysis indicated that the outage performance is only sightly degraded by residual interference related to FD mode but otherwise the outage performance loss can be very substantial as changing the number of transmit antennas at the BS. Furthermore, we observed that target rates have small impact on such outage performance.

REFERENCES

[1] D.-T. Do and M.-S. Van Nguyen, “Device-to-device transmission modes in NOMA network with and without wireless power transfer,” *Computer Communications*, vol. 139, pp. 67-77, May 2019.

[2] D.-T. Do, M. Vaezi, T.-L. Nguyen, “Wireless powered cooperative relaying using NOMA with Imperfect CSI,” *Proc. of IEEE Globecom Workshops (GC Wkshps), Abu Dhabi, UAE*, September 2018.

[3] D.-T. Do, A.-T. Le, "NOMA based cognitive relaying: Transceiver hardware impairments, relay selection policies and outage performance comparison," *Computer Communications*, vol. 146, pp. 144-154.

[4] D.-T. Do, A.-T. Le and B.-M. Lee, "On performance analysis of underlay cognitive radio-aware hybrid OMA/NOMA networks with imperfect CSI," *Electronics*, vol. 8, no.7, July 2019.

[5] X. Li, W. Xu, Z. Feng, X. Lin, and J. Lin, "Matching-theory-based spectrum utilization in cognitive NOMA-OFDM systems," *Proc. IEEE Wireless Commun. Netw. Conf. (WCNC)*, March 2017.

[6] F. Zhou, Z. Chu, H. Sun, and W. C. M. Leung, "Resource allocation for secure MISO-NOMA cognitive radios relying on SWIPT," *Proc. IEEE Int. Conf. Commun., Kansas City*, May 2018.

[7] D. T. Do, A. T. Le, C.-B. Le and B. M. Lee, "On exact outage and throughput performance of cognitive radio based non-orthogonal multiple access networks with and without D2D link," *Sensors*, vol. 19, no. 15, 2019.

[8] D.-T. Do and C.-B. Le, "Application of NOMA in wireless system with wireless power transfer scheme outage and ergodic capacity performance analysis," *Sensors*, vol. 18, no. 10, 2018.

[9] T.-L. Nguyen and D.-T. Do, "Exploiting impacts of intercell interference on SWIPT-assisted Non-orthogonal multiple access," *Wireless Communications and Mobile Computing*, vol. 2018, no.17, pp.1-12, November 2018.

[10] D.-T. Do, M.-S. Van Nguyen, T.-A. Hoang and M. Voznak, "NOMA-assisted multiple access scheme for IoT deployment: relay selection model and secrecy performance improvement," *Sensors*, vol. 19, no.3, February 2019.

[11] P. D. Diamantoulakis, *et al*., "Wireless-powered communications with non-orthogonal multiple access," *IEEE Trans. Wireless Commun*, vol. 15, no. 12, pp. 8422-8436, December 2016.

[12] Y. Liu, Z. Ding, M. Elkashlan, H. V. Poor, "Cooperative nonorthogonal multiple access with simultaneous wireless information and power transfer," *IEEE Journal on Selectrd Areas in Communications*, vol. 34, no. 4, April 2016.

[13] Z. Yang, Z. Ding, P. Fan, N. Al-Dhahir, "The impact of power allocation on cooperative non-orthogonal multiple access networks with SWIPT," *IEEE Trans. Wireless Commun*, vol. 16, no.7, July 2017.

[14] D.-T. Do, *et al.*, "Wireless power transfer enabled NOMA relay systems: two SIC modes and performance evaluation," *TELKOMNIKA Telecommunication Computing Electronics and Control*, vol. 17, no. 6, pp. 2697-2703, December 2019.

[15] D.-T. Do, C.-B. Le and A.-T. Le, "Cooperative underlay cognitive radio assisted NOMA: secondary network improvement and outage performance," *TELKOMNIKA Telecommunication Computing Electronics and Control*, vol.17, no. 5, pp. 2147-2154, October 2019.

[16] D.-T. Do and T.-T. Thi Nguyen, "Exact outage performance analysis of amplify-and forward-aware cooperative NOMA," *TELKOMNIKA Telecommunication Computing Electronics and Control*, vol. 16, no. 5, pp. 1966-1973, October 2018.

[17] D.-T. Do and C.-B. Le, "Exploiting outage performance of wireless powered NOMA," *TELKOMNIKA Telecommunication Computing Electronics and Control*, vol. 16, no. 5, pp. 1907-1917, October 2018.

[18] G. J. Foschini and M. J. Gans, "On limits of wireless communications in a fading environment when using multiple antennas," *Wireless Pers. Commun*, vol. 6, no.3, pp. 311-335, 1998.

[19] I. E. Telatar, "Capacity of multi-antenna Gaussian channels," *Eur. Trans. Telecommun*, vol. 10, no.6, pp. 585-595, 1999.

[20] S. Sanayei, A. Nosratinia, "Antenna selection in MIMO systems," *IEEE Commun. Mag*, vol. 42, no. 10, pp. 68-73, October 2004.

[21] N. B. Mehta, S. Kashyap, and A. F. Molisch, "Antenna selection in LTE: From motivation to specification," *IEEE Commun. Mag. Mag*, vol. 50, no. 10, pp. 144-150, October 2012.

[22] Z. Chen, J. Yuan, and B. Vucetic, "Analysis of transmit antenna selection/maximal-ratio combining in Rayleigh fading channels," *IEEE Trans. Veh. Technol*, vol. 54, no. 4, July 2005.

[23] Y. Zhang, J. Ge, E. Serpedin, "Performance analysis of nonorthogonal multiple access for downlink networks with antenna selection over Nakagami-m fading channels," *IEEE Trans. Veh. Technol*, vol. 66, no.11, November 2017.

[24] Y. Yu, *et al*., "Antenna selection for MIMO nonorthogonal multiple access systems," *IEEE Trans. Veh. Technol*, vol. 67, no. 4, pp. 3158-3171, April 2018.

[25] X. Liu, X. Wang, "Efficient antenna selection and user scheduling in 5G massive MIMO-NOMA system," *Proc. IEEE Veh. Technol*, May 2016.

[26] S. Lee, *et al*., "Outage probability of non-orthogonal multiple access schemes with partial relay selection," *2016 IEEE 27th Annual International Symposium on Personal, Indoor, and Mobile Radio Communications (PIMRC)*, September 2016.

[27] J. Xiong, *et al*., "Wong. Secrecy performance analysis for TAS-MRC system with imperfect feedback," *IEEE Trans. Inf. Forensics Secur*, vol. 10, no.8, August 2015.

[28] M. F. Kader, *et al*., "Duplex non-orthogonal multiple access in cooperative relay sharing for 5G systems," *IEEE Transactions on Vehicular Technology*, vol. 67, no. 7, pp. 5831-5840.